fishes

MDPI

Article

Integrated Analysis of Phenotypic and Hepatic Transcriptomic Profiles Reveals Enhanced Cold Tolerance in Triploid Crucian Carp

Suifei Tao [1,2,†], Zexun Zhou [1,†], Shandong Chen [1,†], Jialin Cui [1], Yude Wang [1], Kaikun Luo [1], Wei Liu [1], Qingfeng Liu [1], Wuhui Li [1,*] and Shaojun Liu [1,*]

[1] Engineering Research Center of Polyploid Fish Reproduction and Breeding of the State Education Ministry, College of Life Sciences, Hunan Normal University, Changsha 410081, China; taosuifei@hnucm.edu.cn (S.T.)
[2] Key Laboratory of Vascula Biology and Translational Medicine, Medical School, Hunan University of Chinese Medicine, Changsha 410208, China
* Correspondence: liwuhui11@163.com (W.L.); lsj@hunnu.edu.cn (S.L.)
† These authors contributed equally to this work.

Abstract

Cold stress poses a critical threat to fish survival by triggering metabolic dysfunction, oxidative damage, immune suppression, and apoptosis. However, hybrid polyploid fish triploid crucian carp (3nRCR, 3n = 150) demonstrate superior stress tolerance. In this study, we investigated the cold adaptation mechanisms in different ploidy cyprinid fishes: triploid crucian carp compared to its diploid improved red crucian carp (*Carassius auratus* red var., RCC, 2n = 100, ♀) and improved allotetraploid (4nAT, 4n = 200, ♂) progenitors. Under controlled cooling, 3nRCR lost equilibrium at a significantly lower temperature (3.2 °C) than RCC (4.0 °C) and 4nAT (4.5 °C), confirming its superior enhanced cold resistance. Histological examination revealed minimal tissue damage in 3nRCR, characterized by reduced gill inflammation and cellular apoptosis. Transcriptomics revealed triploid-specific molecular strategies: 3nRCR uniquely activated retinol metabolism and metabolic rewiring (arginine/proline metabolism, oxidative phosphorylation). Notably, in the immune-related NLR signaling pathway, both *nlrp1* and *nlrp3* (key inflammasome components) were significantly downregulated in 3nRCR ($p < 0.01$). In contrast, genes involved in endoplasmic reticulum (ER) stress response, including *chop* and *nrf2*, were markedly upregulated, indicating a reinforced cellular stress resolution mechanism absent in both RCC and 4nAT. Our results demonstrate that triploid cold adaptation is orchestrated through a balanced interaction among mitochondrial apoptosis, ER stress, and inflammasome pathways. These findings provide novel insights into hybrid polyploid adaptation mechanisms and targets for cold-resilient aquaculture breeding.

Keywords: cold stress; hybrid polyploid fish; histology; transcriptomics; mitochondrial apoptosis; ER (endoplasmic reticulum) stress

Key Contribution: This study pioneers in demonstrating that triploid crucian carp (3nRCR) achieves superior cold tolerance (equilibrium loss at 3.2 °C vs. 4.0–4.5 °C in progenitors) through a unique molecular strategy combining suppressed NLRP inflammasome activation (e.g., *nlrp1*/*nlrp3* downregulation), amplified ER stress adaptation (e.g., *chop*7.2-fold upregulation), mitochondrial apoptosis and metabolic rewiring—revealing a novel mechanism that provides new insights into the molecular mechanisms of heterosis.

Academic Editor: Hélène Volkoff

Received: 7 September 2025
Revised: 2 October 2025
Accepted: 8 October 2025
Published: 12 October 2025

Citation: Tao, S.; Zhou, Z.; Chen, S.; Cui, J.; Wang, Y.; Luo, K.; Liu, W.; Liu, Q.; Li, W.; Liu, S. Integrated Analysis of Phenotypic and Hepatic Transcriptomic Profiles Reveals Enhanced Cold Tolerance in Triploid Crucian Carp. *Fishes* **2025**, *10*, 519. https://doi.org/10.3390/fishes10100519

1. Introduction

Hybrid polyploid adaptation in cyprinid fish represents a critical evolutionary strategy for enhancing environmental stress tolerance, particularly cold resistance—a key determinant of survival in aquatic poikilotherms [1,2]. As ectotherms, fish are highly susceptible to thermal fluctuations due to their direct physiological coupling with ambient water temperatures [3,4]. Temperature critically influences fish growth, reproduction and survival [5], and when it falls below species-specific thresholds, cellular homeostasis is disrupted, leading to metabolic imbalances, immune suppression, and increased mortality [6–8]. Consequently, elucidating the molecular mechanisms underlying cold adaptation in fish has become a major research priority [9].

Thermal stress is further exacerbated during transportation and seasonal harvesting, which amplifies survival risks [10,11]. The ecological and economic significance of cold adaptation are underscored by increasing climate extremes [12]. For example, China's 2022 Orange Cold Wave Warning recorded temperature dropped, exceeding 18 °C within a single event, while the 2008 snow disaster caused water temperature declines of 10–20 °C, devastating southern fisheries [13,14]. These events highlight the urgent need to enhance cold tolerance in aquaculture species [15].

Since the 1980s, the Laboratory of Developmental Biology of Freshwater Fish has conducted hybridization using diploid red crucian carp (2n = 100, ♀) and common carp (2n = 100, ♂) as parental species. Through three generations of hybrid selection, a fertile allotetraploid hybrid (4n = 200) was successfully obtained in the F_3 generation. By continued self-fertilization and propagation, a genetically stable allotetraploid carp-crucian hybrid population (F_3–F_{28}) has been established [16,17]. Utilizing distant hybridization and gynogenesis techniques, improved red crucian carp (RCC) and improved allotetraploid hybrids (4nAT) were developed. By crossing female improved red crucian carp (RCC, 2n = 100, ♀) with male improved allotetraploid hybrids (4nAT, 4n = 200, ♂), a novel improved allotriploid fish—Xiangyun crucian carp 2 (3nRCR, 3n = 150)—was generated. 3nRCR exhibits sterility, making it a safe biological vehicle for transgenic fish production [18,19]. Long-term cultivation studies reveal that 3nRCR exhibits superior adaptability to multiple stressors—including pathogens [20,21], cadmium exposure [22,23], and amino acid deprivation [23]—compared to its diploid (RCC) and tetraploid (4nAT) progenitors. However, the molecular basis of cold tolerance in triploid cyprinids remains unexplored despite their ecological significance [18,24,25].

Given the hepatopancreas's critical role as a central metabolic and immune regulator in teleosts, and its high sensitivity to environmental stressors like thermal extremes [23], we performed transcriptomic analysis on this organ to elucidate hybrid ploidy-specific molecular adaptations to cold challenge.

2. Materials and Methods

2.1. Experimental Design

The experimental fish were obtained from the Polyploid Fish Reproduction and Breeding Engineering Research Center at Hunan Normal University. Three groups were used: 3-month-old 3nRCR (mean body weight = 4.81 ± 0.52 g, body length = 7.12 ± 0.49 cm), their parental diploid RCC (body weight = 3.52 ±0.68 g, body length = 6.2 ± 0.52 cm), and 4nAT (body weight = 3.38 ± 0.57 g, body length = 6.18 ± 0.59 cm). Forty fish were randomly selected from each group. All specimens were maintained under standardized aquaculture conditions at 25 °C and pH 7.0–7.5. They were fed a commercial diet at 2.5% of body weight daily, administered twice daily at 09:00 and 16:00. After a one-week acclimatization period, experiments were conducted under controlled laboratory conditions with the following water parameters: temperature 26 °C, pH 6.4–7.0, and dissolved oxygen 6.0–8.0 mg/L.

Preliminary low-temperature stress experiment: twenty fish from each group, 3nRCR and its parental lines, were tagged. The water temperature was gradually decreased from room temperature (26 °C) at a rate of 1 °C/h. This cooling protocol was chosen based on previous studies that demonstrated the significant impact of temperature changes on fish physiology [25–28]. Temperature regulation was achieved using a chiller (AOLINGHENGYE YSZY-02, Shenzhen, China) with the cooling rate (1 ± 0.2 °C/h) monitored using a precision mercury thermometer (Sanasi Scientific Instrument co., Ltd, JianHu, China). The temperature at which each fish lost equilibrium and rolled over was recorded. Twenty tagged individuals from each group (3nRCR and its two parental species) were subjected to cold stress.

Acute low-temperature stress experiment: The water temperature was gradually reduced from 26 °C to 8 °C at a rate of 1 °C/h, held at 8 °C for 36 h, and then further decreased at the same rate until the fish lost equilibrium and turned over. Observations were recorded every 20 min. Upon reaching 8 °C, fish from each group were randomly sampled. Fish were anesthetized with an appropriate concentration of MS-222 (Sigma-Aldrich, St. Louis, MO, USA), and approximately 0.2 mL of whole blood was collected from the caudal vein using a sterile syringe (Hunan kanglilai medical instrument co., Ltd, Suzhou, China) pre-moistened with acid-citrate-dextrose anticoagulant (Sangon biotech, ShangHai, China). Blood samples were centrifuged at 3000× *g* to isolate plasma for subsequent enzyme activity assays. Liver and gill tissues were rapidly dissected using sterilized tools (Suzhou beiruowei medical instrument co., Ltd, SuZhou, China). Portions of these tissues were immediately frozen for enzyme assays, while the remaining samples were washed in DEPC-treated water, flash-frozen in liquid nitrogen, and stored at –80 °C for transcriptome analysis. Additionally, pieces of liver, gill, and intestine tissues were fixed in 4% paraformaldehyde for histological examination. Three biological replicates were included for each group at each temperature point for transcriptome and qPCR analyses.

2.2. Histopathology Assay

Liver and gill tissues were fixed in 4% paraformaldehyde overnight, followed by paraffin embedding for tissue sectioning. Serial sections (3–4 μm thick) were prepared using a rotary microtome(Shanghai Leica Instrument Co., Ltd, Shanghai, China). Tissue sections were stained with hematoxylin and eosin (H&E) following standard protocols [29]. Complete sections of different tissues were examined under a light microscope (Motic (Xiamen) electric group co., Ltd., Xiamen, China) at magnifications of 4×, 10×, 20×, and 40× to observe the tissue structures and were photographed for records.

2.3. Hepatopancreas Transcriptome Sequencing and Analysis

Total RNA was extracted from hepatopancreas tissues (n = 3 per group) using TRIzol reagent (Thermo Fisher Scientific Inc, Waltham, MA, USA). RNA samples with an RNA Integrity Number (RIN) ≥8.0, as assessed by an Agilent 2100 Bioanalyzer (Agilent Technologies, Santa Clara, CA, USA), were used for library preparation. The cDNA libraries were sequenced on an Illumina HiSeq 4000 platform (150 bp paired-end reads) by Biomarker Technologies (Beijing, China).

Bioinformatic analyses were conducted on the BMKCloud platform (www.biocloud.net)(access on 25 August 2025). After filtering raw reads to obtain clean data, reads were aligned to the Carassius auratus reference genome (v.Ca1). Gene expression was quantified as FPKM. Differentially expressed genes (DEGs) were identified with thresholds of $|\log_2(\text{FoldChange})| \geq 1$ and a false discovery rate (FDR) <0.05. Functional annotation of DEGs was performed against Nr, Swiss-Prot, KEGG, and COG databases

(E-value < 1×10^{-5}). Gene Ontology (GO) and KEGG pathway enrichment analyses were performed, with a corrected p-value < 0.05 considered significant.

2.4. Quantitative Real-Time PCR (qRT-PCR) Validation

Eight DEGs and five genes in Ko04141 were selected for qRT-PCR validation. Gene-specific primers were designed using Primer Premier 5.0 software (Tables S1 and S2). QRT-PCR assays were performed in triplicate with SYBR Green PCR Master Mix (Applied Biosystems, Thermo Fisher Scientific Inc, Waltham, MA, USA) on an ABI 7500 Real-Time PCR System (Applied Biosystems, Thermo Fisher Scientific Inc, Waltham, MA, USA). The relative expression levels of target genes were calculated using the $2^{-\Delta\Delta Ct}$ method with β-actin as the endogenous reference gene.

2.5. Statistical Analysis

All data are presented as means ± standard deviation (SD). Differences between groups were assessed using Student's t-test or one-way analysis of variance (ANOVA), followed by Duncan's multiple range test for post-hoc comparisons. A threshold of $p < 0.05$ was applied to determine statistical significance. Analyses were conducted using SPSS 27 (IBM, Armonk, NY, USA) [21].

3. Results

3.1. Triploid 3nRCR Exhibits Superior Behavioral Cold Tolerance During Gradual Cooling

In our preliminary experiment, the 4nAT strain first exhibited loss of equilibrium, characterized by lateral rolling behavior, at 6.6 ± 0.2 °C. RCC displayed similar stress responses at 6.0 ± 0.2 °C, while 3nRCR demonstrated superior cold resistance, maintaining equilibrium until 5.1 ± 0.3 °C. During the formal experiment, under controlled cooling conditions (1 °C/h from 26 °C, Figure 1), 3nRCR maintained equilibrium until 3.2 ± 0.3 °C, significantly lower than 4.0 ± 0.3 °C in RCC and 4.5 ± 0.2 °C in 4nAT. This superior cold tolerance aligned with reduced tissue damage, as evidenced by minimal gill inflammation and hepatocytes apoptosis in 3nRCR (Figures 2H and 3D), contrasting with severe pathology in 4nAT (Figures 2L and 3F) and RCC (Figures 2D and 3B). This leads to various pathological changes in different tissues, including crystal formation, necrosis, and shock. These results demonstrated that 3nRCR possesses significantly greater innate cold resistance than its parental strains. In addition, acclimation at 8 °C improved cold tolerance in all groups. The hierarchical order of cold resistance (3nRCR > RCC > 4nAT) remained consistent both before and after acclimation.

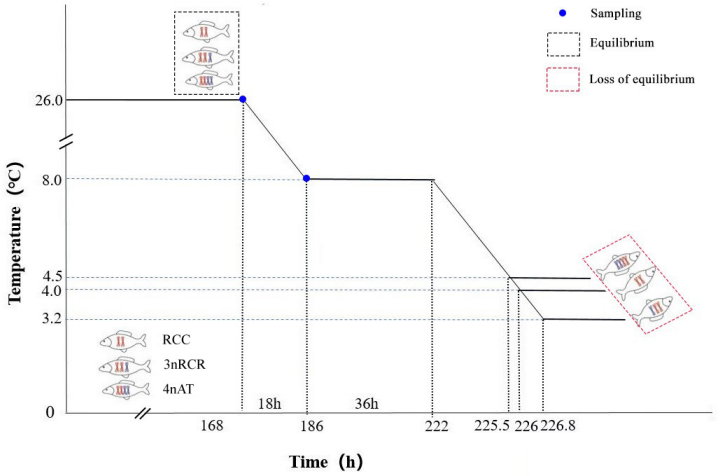

Figure 1. Flowchart of the cold stress in 3nRCR and its parents that have been cold domesticated at 8 °C and cooled down sharply to the loss of equilibrium (LOE). (red and blue indicate chromosomes originating from different parents).

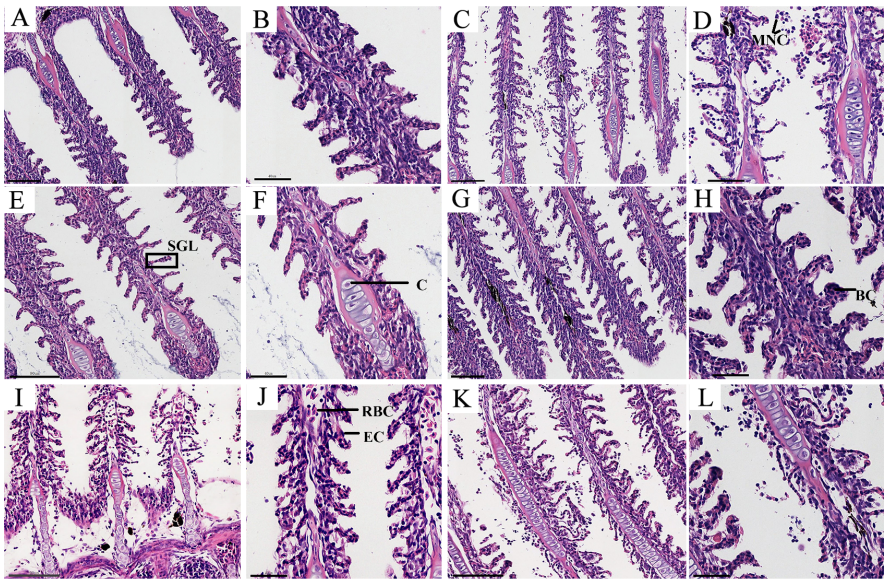

Figure 2. Hematoxylin-eosin staining of gill tissue from 3nRCR and its parents under normal and cold stress conditions. (**A**,**C**): RCC gill tissue at 26 °C, 8 °C; (**E**,**G**): 3nRCR gill tissue at 26 °C, 8 °C; (**I**,**K**): 4nAT gill tissue at 26 °C, 8 °C; bars = 90 μm. (**B**,**D**): local enlargements of (**A**,**C**); (**F**,**H**): local enlargements of (**E**,**G**); (**J**–**L**): local enlargements of (**I**–**K**); bars = 40 μm. SGL: Secondary gill lamellae; BC: Blood cell; MNC: Mononuclear Cell; RBC: Red blood cell; EC: Epithelial cell; C: Chondrocyte.

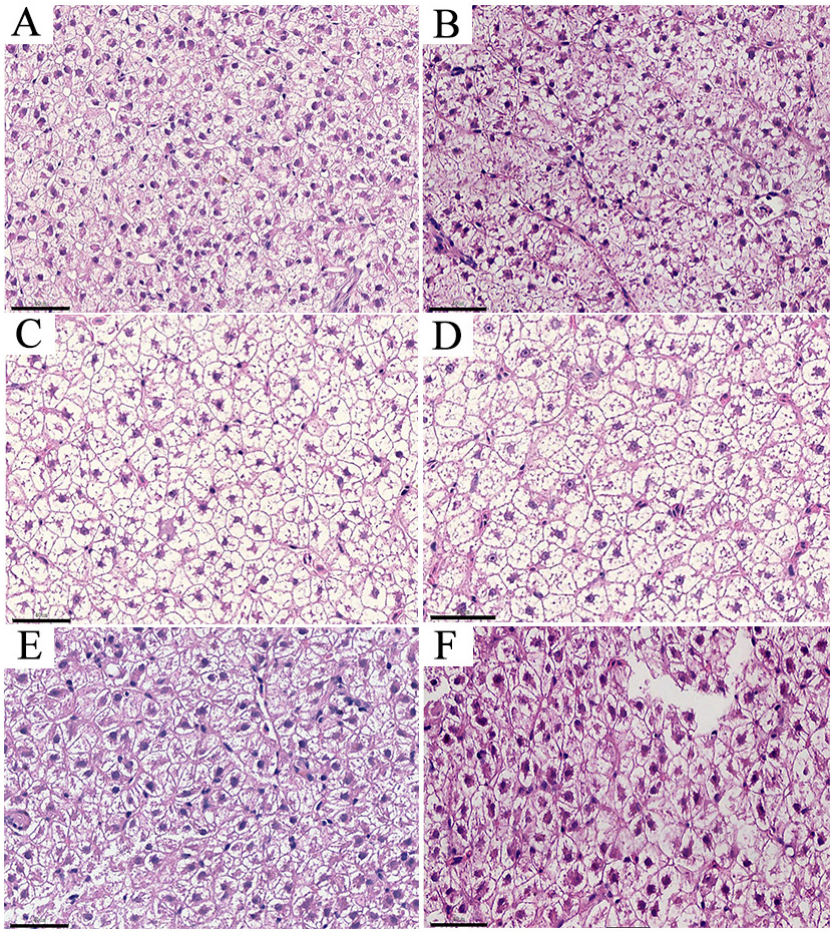

Figure 3. Hematoxylin-eosin staining of liver tissue from 3nRCR and its parents under normal and cold stress conditions. (**A**,**B**): RCC liver tissue at 26 °C, 8 °C; (**C**,**D**): 3nRCR liver tissue at 26 °C, 8 °C; (**E**,**F**): 4nAT liver tissue at 26 °C, 8 °C; bars = 40 μm.

3.2. Gill and Liver Histopathology Reveals Ploidy-Dependent Tissue Damage and Inflammation

Microscopic analysis revealed distinct ploidy-specific patterns of tissue damage in gill and liver exposed to 8 °C cold stress. Under normal temperature, the secondary lamellae of gills remained intact in both 3nRCR and RCC (Figure 2A,E). In 4nAT, most lamellae were also intact (Figure 2J), though minor leukocyte infiltration was observed (Figure 2I), suggesting that 4nAT may be more susceptible to environmental fluctuations under normal conditions. In the 8 °C low-temperature group, significant hemorrhage—particularly MNC (mononuclear cell) infiltration—and fragmentation of the secondary lamellae were evident in both parental RCC and 4nAT (Figure 2D,L), indicating that cold stress induced marked inflammatory responses and compromised the structural integrity of the gill barrier. In contrast, the secondary lamellae of triploid 3nRCR remained largely intact under cold stress (Figure 2H). However, an expansion of the interlamellar cell mass (ILCM) was observed, accompanied by widening of the lamellae and an increased accumulation of hemocytes within them. Apoptotic cell aggregation may also be present. These morphological adaptations suggest that the gill tissue of 3nRCR sustained less severe damage compared to the parental lines under low-temperature stress.

In the normal group, the nuclei of hepatic cells were evenly distributed and centrally located within the cells (Figure 3A,C,E) At 8 °C, the nuclei in the RCC group became relatively condensed, indicating partial nuclear dissolution (Figure 3B). In 3nRCR, cell contours remained distinct, nuclei were evenly distributed, and no dissolution was observed (Figure 3D). The hepatocytes of 4nAT displayed swelling, partial nuclear dissolution, and increased eosinophilia (suggesting denser cytoplasm) (Figure 3F). The occurrence of apoptosis in the gill and liver of 3nRCR is also likely, a possibility that requires further validation through specific apoptosis assays such as TUNEL staining.

The histological findings corroborate the behavioral data: 3nRCR shows the least structural damage and inflammation in both gill and liver tissues under cold stress (Figures 2H and 3D), while 4nAT exhibits the most severe pathology (Figures 2L and 3F), RCC displayed an intermediate level of damage (Figures 2D and 3B). The reduced histopathological damage in 3nRCR (Figures 2H and 3D) aligned with its unique transcriptomic reprogramming described below.

3.3. Transcriptomic Profiling Identifies Triploid-Specific Stress Adaptation Networks in Hepatopancreas

3.3.1. Global Transcriptional Changes and Quality Control

Hepatopancreas transcriptomes yielded 118.91 Gb clean data from 18 samples (3nRCR, RCC, 4nAT at 26 °C and 8 °C; $n = 3$ per group per temperature). Analysis revealed 5123 new genes, with 2330 functionally annotated (Table S3).

3.3.2. Alternative Splicing Dynamics Highlight Transcriptional Stability in Triploids

Cold stress induced distinct patterns of alternative splicing (AS) events across ploidy types (Figure S1). In RCC (diploid) at 26 °C, 48,978 alternative splicing events were detected; this increased to 51,785 at 8 °C. In 4nAT (tetraploid), the number increased from 32,733 at 26 °C to 45,529 at 8 °C. However, in 3nRCR (triploid), the number decreased from 43,865 at 26 °C to 40,646 at 8 °C. This indicates that cold stress significantly increased AS complexity (splicing burden) in diploid and tetraploid fish but paradoxically reduced it in the triploid 3nRCR, suggesting enhanced transcriptional stability under stress.

3.3.3. Functional Enrichment Reveals Ploidy-Specific Pathways

Comparative analysis of gene expression between 8 °C (cold stress) and 26 °C (control) revealed significant ploidy-dependent differences in the number of differentially expressed

genes (DEGs, $|\log_2 FC| \geq 1$, FDR < 0.05). 3nRCR exhibited the most extensive transcriptional reprogramming, with 3755 DEGs (1665 upregulated and 2090 downregulated under cold stress). RCC showed 1776 DEGs (1132 upregulated, 644 downregulated). 4nAT displayed the least response, with only 828 DEGs (452 upregulated and 376 downregulated).

Venn analysis identified delineated 2974 unique DEGs specific to 3nRCR under cold stress (Figure 4A), representing 79.2% of its total DEGs. Gene Ontology (GO) analysis (Figure 4B) indicated these unique triploid transcripts were significantly enriched in core functional categories related to cellular processes, stress response and immune regulation. KEGG pathway classification (Figure 4C) further identified the immune related pathway-Herpes simplex virus 1 infection as the most significantly enriched pathway among 3nRCR, containing 57 DEGs. Among these, 39 genes were downregulated and 18 genes were upregulated at 8 °C.

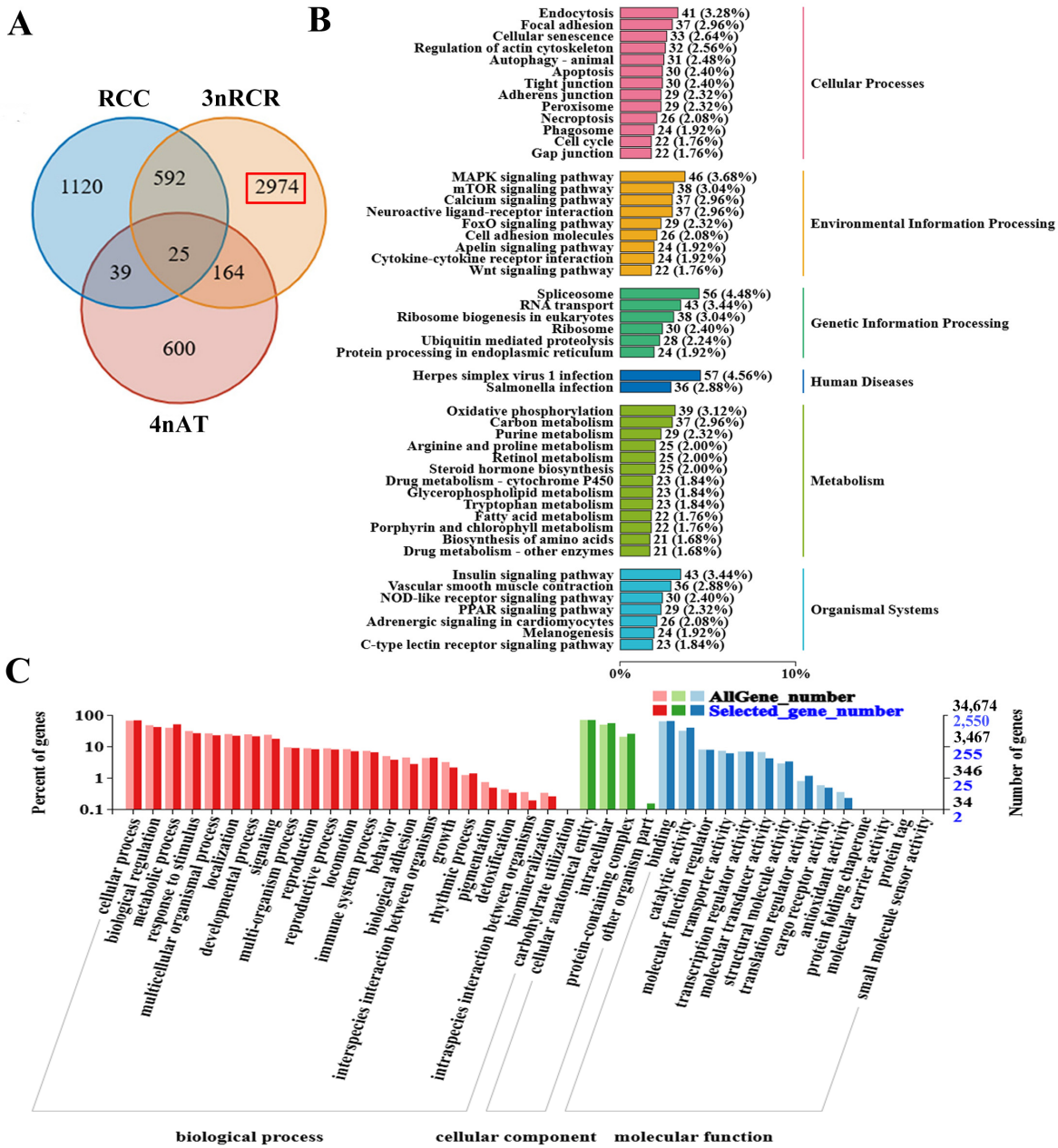

Figure 4. Venn diagram (**A**) of DEGs in 3nRCR and its parents, GO analysis (**B**) and KEGG enrichment analysis (**C**) of unique DEGs in 3nRCR. The red square in (**A**) identifies 2974 unique DEGs in the 3nRCR under cold stress.

3.4. Validation of Gene Expression by qRT-PCR

To validate the transcriptomic profiling results, we quantified the expression of eight key genes (*tlr3*, *tlr5*, *bcl2l1*, *bax*, *nfkbia*, *nlrp3*, *cytc*, *nrf2*) in RCC, 3nRCR, and 4nAT under cold stress (8 °C *vs.* 26 °C) using qRT-PCR. Comparing the 26 °C group with the 8 °C group, qRT-PCR validation of eight target genes demonstrated high concordance with RNA-seq data (Figure 5), confirming the reliability of transcriptome profiling under cold stress (8 °C vs. 26 °C). Specifically, *tlr3* expression was exclusively downregulated in RCC and 3nRCR ($p < 0.01$) but exhibited no statistically significant differences in 4nAT. Both *tlr5*, *bax* and *bcl2l1* exhibited significant upregulation in 3nRCR ($p < 0.05$), but exhibited no statistically significant differences in RCC and 4nAT. The NF-κB inhibitor *nfkbia* was upregulated in 3nRCR ($p < 0.01$), whereas the inflammasome gene *nlrp3* was markedly downregulated ($p < 0.001$). Mitochondrial apoptosis marker *cytc* showed upregulation across all strains (RCC, 3nRCR, 4nAT; $p < 0.05$), and antioxidant regulator *nrf2* was elevated in 3nRCR ($p < 0.05$). In addition to *nlrp3* downregulation, *nlrp1*—a key inflammasome sensor for viral pathogens—showed significantly reduced expression ($p < 0.001$) in 3nRCR, whereas its expression levels in RCC and 4nAT exhibited no statistically significant differences according to transcriptome data (Figure 5). This coordinated suppression of NLR inflammasomes suggests a triploid-specific strategy to attenuate pyroptosis and redirect energy toward stress adaptation. These results underscore triploid 3nRCR's unique molecular adaptation via suppressed inflammation (*nlrp1*↓, *nlrp3*↓) and enhanced stress resilience (*bcl2l1*↑, *nrf2*↑).

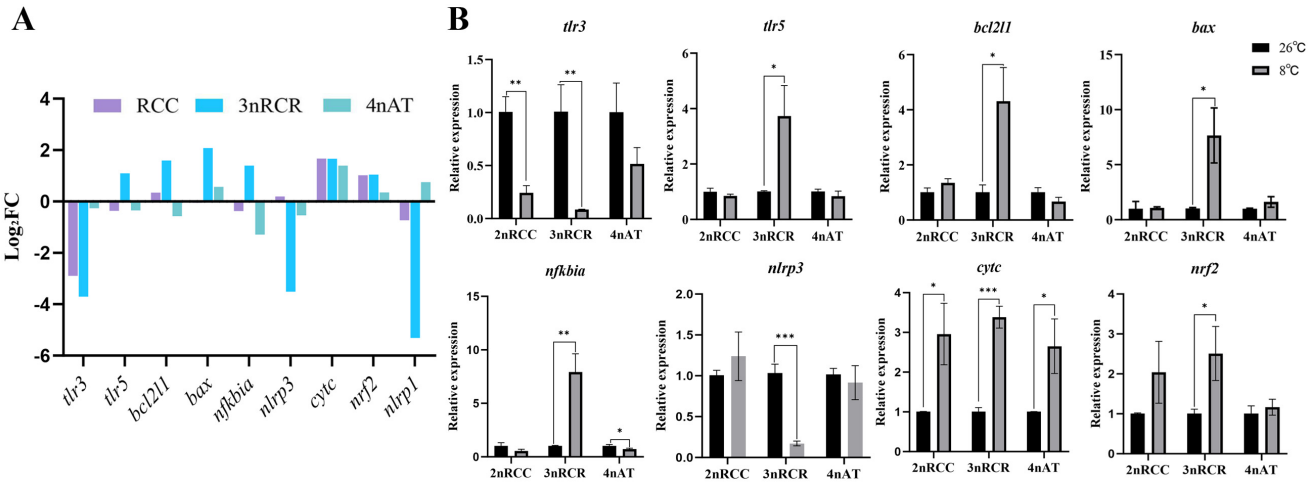

Figure 5. Transcriptome (the figure (**A**) shows the FPKM values of the transcriptome) and qPCR expression plots of DEGs under cold stress in 3nRCR and their parents (**B**). * denotes $p < 0.05$, ** denotes $p < 0.01$, *** denotes $p < 0.001$.

3.5. Differential Gene Expression and Functional Annotation-ER Stress-Immune Crosstalk Differentiates Survival Strategies

Comparative transcriptomic analysis of triploid 3nRCR and its diploid (RCC) and tetraploid (4nAT) parents under cold stress (8 °C vs. 26 °C) revealed heterosis-dependent transcriptional reprogramming. Gene Ontology (GO) analysis indicated that 3nRCR exhibited predominant downregulation of genes in key functional categories (cellular processes, response to stimulus, immune system processes, molecular function regulation, and transporter activity), suggesting adaptive modulation of immune signaling, transcription, and stress response pathways. In contrast, RCC and 4nAT showed upregulation dominance in these categories, highlighting divergent survival strategies (Figure S2). KEGG pathway enrichment further demonstrated distinct molecular adaptations: 3nRCR was uniquely enriched in Herpes simplex virus 1 infection, alongside exclusive metabolic pathways in-

cluding arginine/proline metabolism, histidine metabolism, fatty acid metabolism, retinol metabolism, and oxidative phosphorylation—all absent in parental top-enriched pathways. 3nRCR's co-enrichment of viral defense and metabolic reprogramming points to a coordinated immune-metabolic adaptation (Figures S3 and 6).

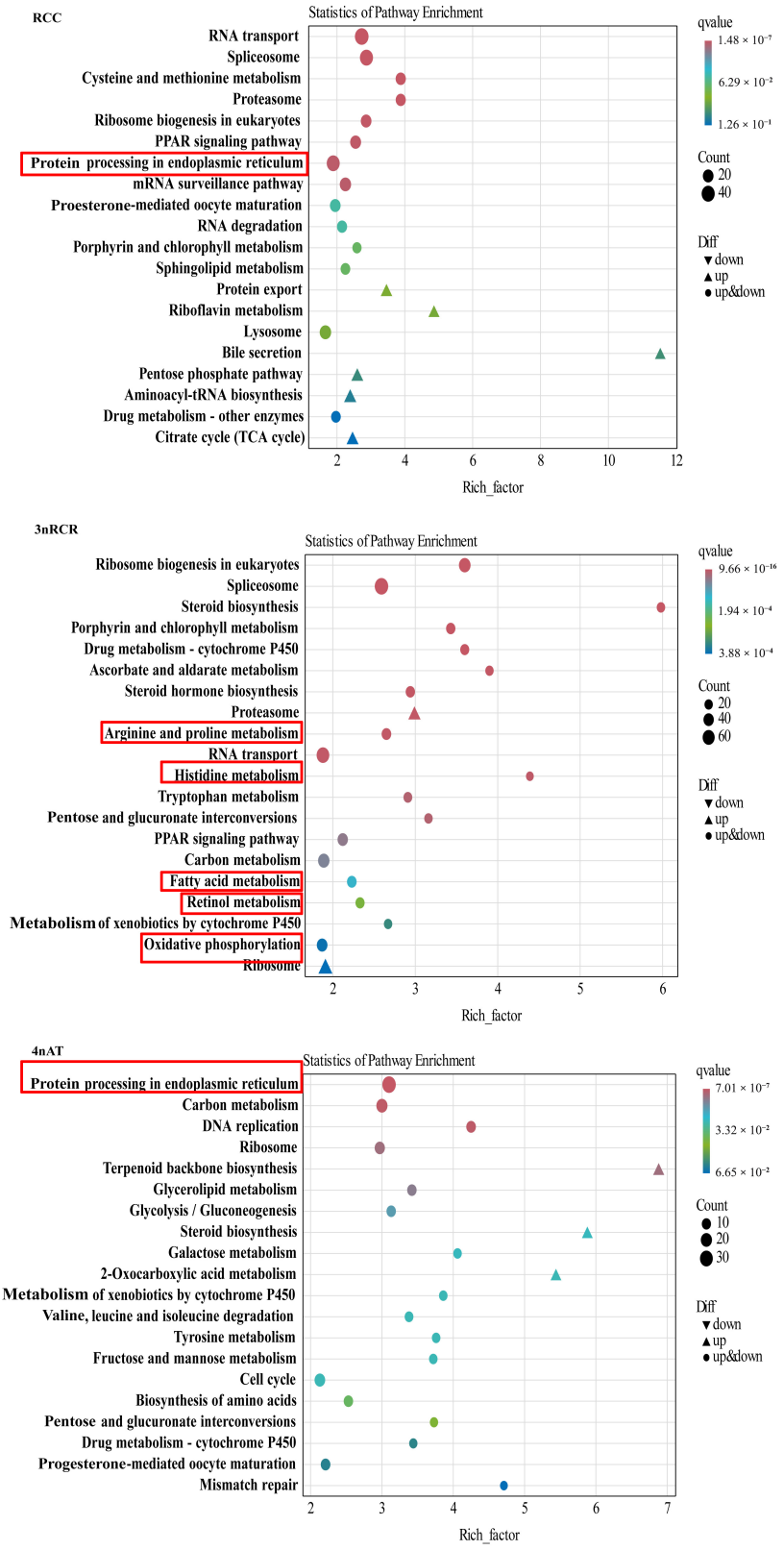

Figure 6. KEGG enrichment of DEGs under cold stress in 3nRCR and their parents.

Transcriptional profiling revealed significant enrichment of apoptosis and immune-related signaling pathways in triploid 3nRCR under cold stress. Specifically, mitochondrial apoptosis pathway genes exhibited ploidy-dependent regulation: *bax* (pro-apoptotic) was significantly upregulated in 3nRCR ($p < 0.05$), whereas *chop* (endoplasmic reticulum stress-induced apoptosis mediator) was exclusively upregulated in 3nRCR ($p < 0.0001$). Concurrently, *nfkbia* (encoding IκBα, an inhibitor of NF-κB inflammatory signaling) was markedly elevated in 3nRCR ($p < 0.01$) but suppressed in 4nAT ($p < 0.05$), while it exhibited no statistically significant differences in RCC, indicating triploid-specific suppression of inflammatory responses and potential redirection of energy toward stress adaptation.

The immune-related NOD-like receptor (NLR) signaling pathway displayed ploidy-specific divergence (Figure 7). Triploid 3nRCR exhibited substantially more differentially expressed genes (DEGs) in this pathway compared to diploid RCC and tetraploid 4nAT. Notably, both *nlrp1* and *nlrp3*—core inflammasome sensors that indicate *caspase*-1-dependent pyroptosis and *il-1β* maturation—were significantly downregulated in 3nRCR ($p < 0.001$), whereas no significant changes occurred in parental strains. This coordinated suppression of inflammasome components (*nlrp1*/*nlrp3*) and concomitant upregulation of *nfkbia* (an inhibitor of NF-κB signaling) suggests a triploid-specific strategy to attenuate inflammation-driven tissue damage under cold stress. Mechanistically, *nlrp1* deficiency may reduce pyroptotic cell death by limiting *caspase-1* activation, while *nlrp3* downregulation curbs IL-1β-driven inflammation. Concurrently, the promotion of mitochondrial apoptosis provides a controlled alternative for cell removal, thereby maintaining tissue homeostasis without exacerbating inflammatory cascades.

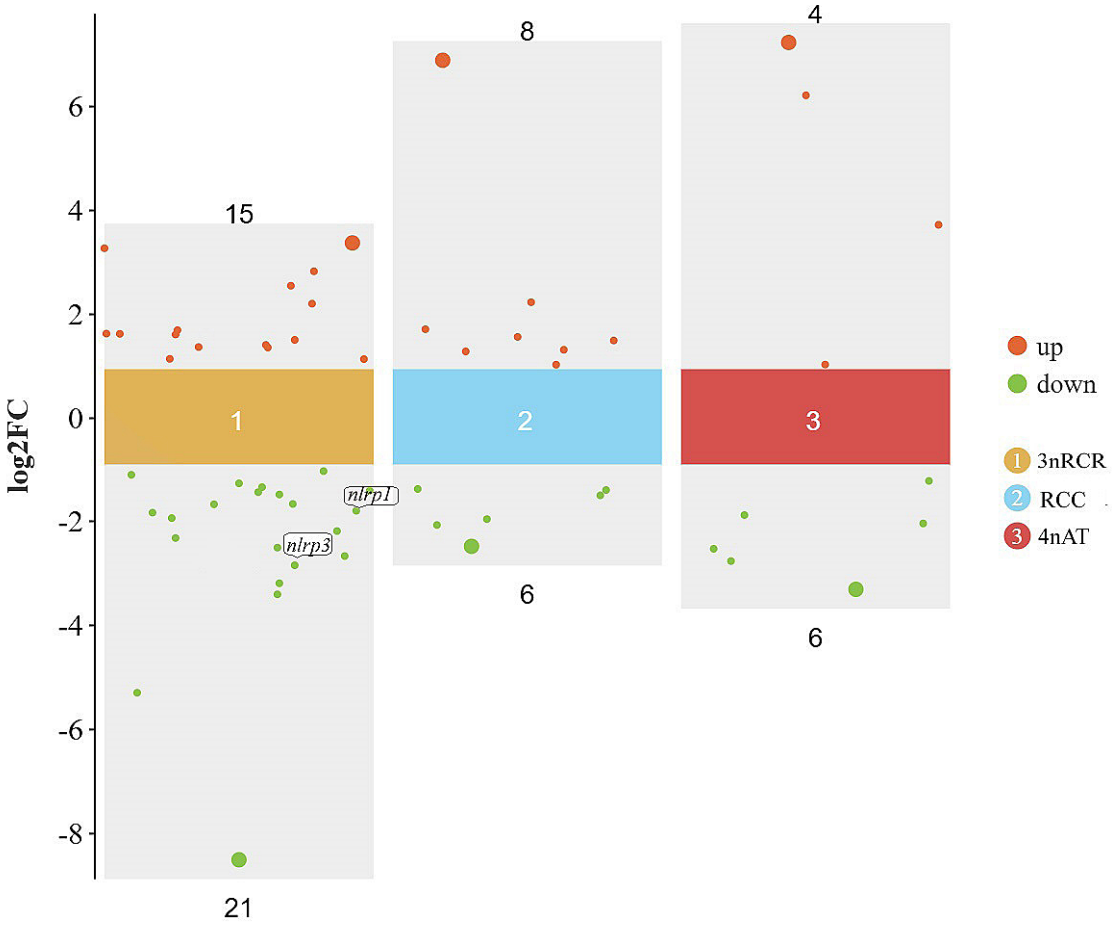

Figure 7. Differentially expressed genes in the NLR signaling pathway under acute low-temperature stress in 3nRCR and its parental species.

Transcriptional profiling of the immune-related Toll-like receptor (TLR) signaling pathway under acute low-temperature stress revealed ploidy-specific differential regulation in triploid 3nRCR and its diploid (RCC) and tetraploid (4nAT) parents. Triploid 3nRCR exhibited the most pronounced response, with 11 differentially expressed genes (DEGs). Notably, membrane-bound *tlr5* (recognizing bacterial flagellin) was significantly upregulated in 3nRCR ($p < 0.05$), while intracellular *tlr3* (sensing viral dsRNA) was exclusively downregulated ($p < 0.01$). This divergence suggests a triploid-specific strategy to enhance extracellular pathogen surveillance while suppressing intracellular viral defense mechanisms under cold stress.

Transcriptomic analysis revealed significant activation of the endoplasmic reticulum (ER) stress pathway (KEGG Ko04141) in 3nRCR, characterized by coordinated upregulation of key mediators in the PERK-eIF2α-ATF4 signaling axis ($p < 0.05$). Critical components—*perk* (eukaryotic translation initiation factor 2-alpha kinase 3), *eif2s1* (encoding eIF2α), *ppp1r15a* (encoding GADD34), and the pro-apoptotic transcription factor *chop* (*ddit3*)—were significantly elevated ($p < 0.05$), indicating robust induction of the integrated stress response (ISR). Quantitative real-time PCR (qRT-PCR) validated these findings, confirming significant overexpression of five core ER stress genes (*perk*, *eif2α*, *gadd34*, *chop*, *nrf2*) in 3nRCR (Figure 8B). Notably, 3nRCR exhibited amplified stress resolution capacity compared to diploid controls (RCC): *Nrf2* induction reached 2.5-fold (vs. 2.0-fold in RCC), enhancing antioxidant defenses, while *chop* expression surged 7.2-fold (vs. 3.7-fold in RCC), reflecting heightened ER stress sensitivity alongside potential GADD34-mediated feedback regulation. In contrast, 4nAT showed downregulation of *perk* and *eif2α* based on RNA-seq data, suggesting impaired PERK-dependent translational control that may contribute to dysregulated stress adaptation in tetraploid systems. The concomitant upregulation of *nrf2* ($p < 0.05$) further underscores ISR activation to mitigate proteotoxic damage in 3nRCR—a triploid-specific adaptation via ER proteostasis remodeling, distinct from parental strains (RCC/4nAT) where ER stress genes were unaltered or suppressed.

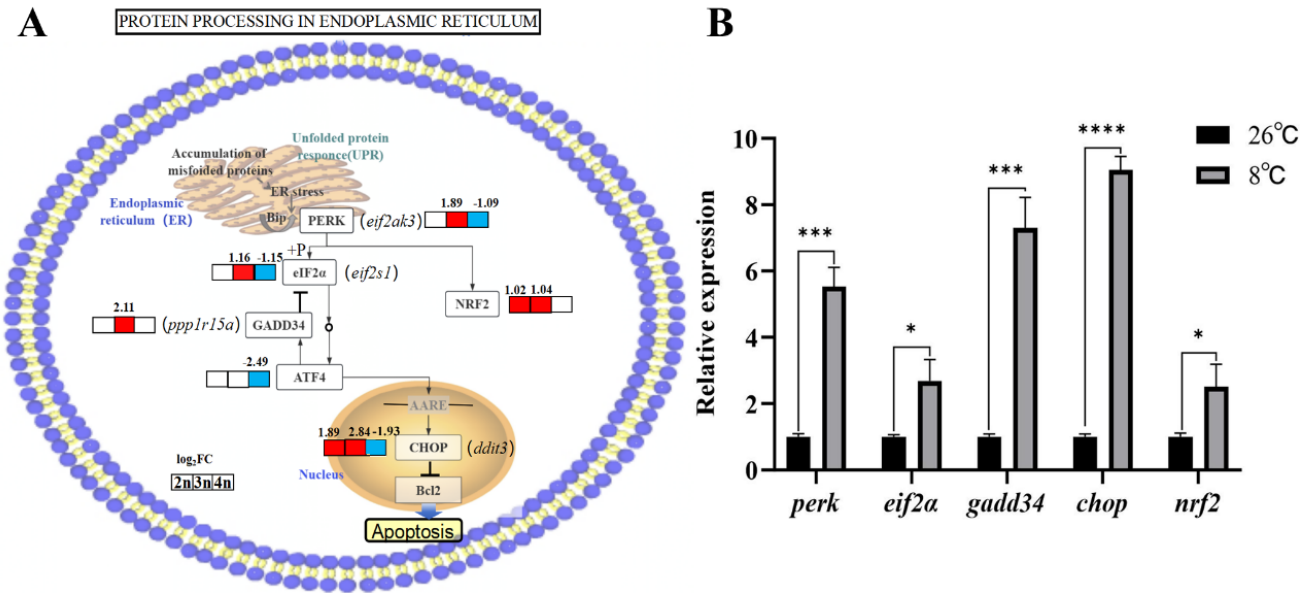

Figure 8. Differentially expressed genes in the Ko04141 signaling pathway under acute low-temperature stress in 3nRCR and its parental species. (**A**): KEGG map of the signaling pathway of DEGs with the genes of interest for our study in Ko04141 under cold stress of in 3nRCR (3n) and its parental species RCC(2n)/4nAT(4n) (Up-regulated expressed genes in red and down-regulated expressed genes in blue). (**B**): The qPCR expression plots of the interested genes in Ko04141 under cold stress in 3nRCR. * denotes $p < 0.05$, *** denotes $p < 0.001$, **** denotes $p < 0.0001$.

4. Discussion

Studies have shown that there are significant differences in cold tolerance among various fish species [28,30]. In studies on acute low-temperature stress, different cooling rates have been employed, such as 0.3 °C/min and 1 °C/h. Although the critical thermal minimum (CTMin) determined at a cooling rate of 0.3 °C/min is widely used, this method may overestimate the thermal limits of larger fish due to the thermal inertia associated with body size and surface area, potentially leading to results that deviate from actual conditions [31–33]. In this study, a relatively moderate acute low-temperature stress treatment method (1 °C/h) was adopted. Our integrated analysis reveals distinct cold adaptation strategies among cyprinid fishes of varying ploidy, with triploid 3nRCR demonstrating superior cold tolerance compared to its diploid (RCC) and allotetraploid (4nAT) progenitors. While our observation that the triploid hybrid (3nRCR) exhibits enhanced cold tolerance is consistent with the heterosis reported by Zhu et al. [34], a key distinction exists in the level of this advantage. In the study by Zhu et al., the hybrid's tolerance was intermediate, surpassing the paternal parent but remaining lower than the maternal parent [34]. In contrast, our 3nRCR demonstrates a stronger, transgressive heterosis, with a low-temperature tolerance that exceeds that of both parental lines.

The behavioral and histological data collectively indicate that 3nRCR maintains tissue integrity and equilibrium at significantly lower critical temperatures (3.2 °C vs. 4.0–4.5 °C in parents), aligning with hepatocytic vacuolar and hydropic degeneration and mononuclear cell infiltration between the gill filaments and lamellae [29] (Figures 2 and 3). The phenomenon of temperature-induced gill remodeling in fish was first documented in the crucian carp *(Carassius carassius*) by Sollid et al. [35]. Under cold but oxygen-rich conditions, interlamellar cell masses (ILCMs) form between the gill lamellae. This proliferation of ILCMs is thought to reduce the functional surface area available for gas and ion exchange, thereby compromising the fish's respiratory and osmoregulatory capacities [36]. Similarly, Chen et al. observed gill structural remodeling in tilapia exposed to 12 °C (a sublethal temperature), characterized by increased ILCMs and morphological irregularities in the secondary lamellae [29]. In our study, the changes observed in triploid 3nRCR under cold stress align with these findings. In contrast, the parental lines exhibited significant inflammatory responses, which we attribute to acute low-temperature exposure triggering immune reactions along with associated cellular damage and death.

The phenotypic advantages are underpinned by a unique molecular architecture, as revealed by transcriptomic profiling, which highlights 3nRCR's exceptional ability to orchestrate CHOP-mediated ER stress resolution [37], suppress NLRP3 inflammasome activation [38], and rewire metabolic pathways to sustain homeostasis under cold duress [9]. It is noteworthy that ploidy variation itself may influence baseline gene expression levels due to genomic dosage effects [1]. However, the observed differential expression patterns (e.g., amplified induction of *chop* and *nrf2* in 3nRCR) likely reflect functional adaptations rather than mere dosage increments, as tetraploids (4nAT) did not show similar upregulation. This suggests that triploidy may facilitate a unique transcriptional landscape that enables more effective stress signaling coordination. Triploidy likely confers genomic buffering capacity, as evidenced by reduced alternative splicing burden under cold stress (Figure S1). This transcriptional stability, combined with ER stress-inflammasome crosstalk, mitochondrial apoptosis, enables efficient resource allocation—prioritizing metabolic rewiring (e.g., OXPHOS—Oxidative Phosphorylation) over costly immune responses [39], ultimately enhancing cold resilience.

4.1. Ploidy-Specific Transcriptional Remodeling and Genomic Flexibility

The triploid's transcriptional response to cold stress diverged markedly from its progenitors, with 3755 DEGs in 3nRCR versus 1776 in RCC and 828 in 4nAT. Notably,

3nRCR exhibited a reduction in alternative splicing events under cold stress, reflecting that the hybrid fish 3nRCR exhibits a faster response capability to cold stress at the molecular level (Figure S1). Under cold stress, alternative splicing (AS) is rapidly initiated in both zebrafish [9] and the hybrids of *Argopecten scallops* [33], consistent with the pattern observed in the RCC and 4nAT. Interestingly, however, AS activity was significantly downregulated in our triploid hybrid 3nRCR. This presents a compelling and meaningful direction for investigating the enhanced cold tolerance mechanisms in hybrid polyploid fish. This may suggest enhanced transcriptional stability in the triploid, possibly minimizing energy expenditure on mRNA processing and favoring efficient translation of stress-responsive proteins—a strategic advantage for rapid cold adaptation.

4.2. ER Stress and Apoptosis: Balancing Survival and Damage Control

The protein processing pathway in the endoplasmic reticulum (ER) was among the top seven most significantly enriched pathways in RCC and 4nAT, and it was the most significantly enriched pathway in 4nAT. However, it did not appear in the top 20 most significantly enriched pathways in 3nRCR. In this pathway, we found that the *chop* gene was highly expressed in 3nRCR and RCC (7.2-fold in 3nRCR vs. 3.7-fold in RCC) but lowly expressed in 4nAT. CHOP is a transcription factor involved in regulating various biological processes and stress responses [37]. Under cellular stress, the expression of *chop* is upregulated. *Chop* plays a key role in the ER stress response, which is triggered by ER dysfunction [37]. *Chop* regulates key molecules in the ER stress pathway, such as *perk*, *ire1α*, and *atf6*, and participates in the regulation of ER stress [39]. CHOP can recruit death ligands such as Fas, TNF-α, and Trail to activate the extrinsic apoptotic receptor, leading to the activation of *caspase-8* and downstream *caspase-3*, thereby inducing apoptosis [39,40]. Huang et al. discovered that under heat stress, largemouth bass (*Micropterus salmoides*) triggers cell apoptosis by inducing ER stress through the CHOP pathway [41]. The upregulation of *chop* in 3nRCR potentially exacerbates cellular apoptosis, which in turn drives the aggregation of apoptotic cells within the gill lamellae and the hepatopancreas observed in histological analyses (Figures 2H and 3D). We speculate that the differential expression of the *chop* gene is closely related to the stronger cold tolerance of 3nRCR compared to its parents, as it may mediate apoptosis through ER stress. As a key transcription factor in ER stress-induced apoptosis [42], the upregulation of *chop* in 3nRCR (Figure 7) likely confers protection by coordinating ER stress resolution, whereas the lack of upregulation in 4nAT correlates with dysregulated PERK-eIF2α signaling. The upregulation of *chop* in RCC is lower than 3nRCR indicated adaptations that were limited in RCC. CHOP may play a protective role in 3nRCR by balancing pro-survival and pro-apoptotic signals [38]. This is further supported by the differential expression of other ER stress markers: *eif2α* and *nrf2* (2.5-fold vs. 2.0-fold in RCC) were upregulated in 3nRCR, but *eif2α* was downregulated in 4nAT, indicating more effective ER stress adaptation in the triploid. Yuan et al. [43] observed differences in eIF2α protein and its phosphorylation levels between triploid Xiangyun crucian carp and diploid red crucian carp, our present study only conducted analyses at the transcriptional level; thus, the results may not be entirely consistent. Such discrepancies could arise from post-transcriptional regulatory mechanisms, such as protein-level mediated by the PERK pathway—e.g., translation inhibition and selective gene expression triggered by eIF2α phosphorylation. Therefore, future investigations should integrate proteomic and phosphoproteomic technologies to further validate and deeply explore the molecular mechanisms of ER stress responses in hybrid polyploid fish at the protein and protein modification levels [44]. Triploid-specific *chop* upregulation (Figure 8 likely orchestrates a protective UPR (unfolded protein response) response, whereas in 4nAT, it correlates with dysregulated PERK-eIF2α signaling—a key vulnerability in tetraploids [37]. How-

ever, our transcriptomic data alone cannot confirm whether CHOP activation in 3nRCR promotes survival or merely delays apoptosis. P53, a pivotal tumor suppressor gene, primarily localizes in the nucleus and induces apoptosis through tissue-specific mechanisms [45]. As a transcriptional activator of the *bax* gene, *p53* enhances *bax* expression. BAX is one of the Bcl-2 family proteins which are key regulators of mitochondrial membrane permeability [45]. Researchers have conducted extensive studies on the changes in mitochondria under low-temperature stress [46–48]. The results from the low-temperature stress experiments revealed that elovl1a$^{-/-}$ and elovl1b$^{-/-}$ zebrafish mutants exhibited aggravated hepatic oxidative stress, mitochondrial metabolic dysfunction, and reduced survival rates under cold conditions [48]. Liu et al. discovered that under chronic cold stress, the expression levels of *p53*, *caspase-8*, and *caspase-9* significantly increased in the liver of juvenile hybrid sturgeon (Acipenser baerii ♀× A. schrenkii ♂) [49], indicating that cold stress induces apoptosis through the *p53*-caspase cascade. This finding is consistent with research on low-temperature stress in tilapia (*Oreochromis niloticus*), pufferfish (*Takifugu obscurus*), juvenile cobia (*Rachycentron canadum*) and orange-spotted grouper (*Epinephelus coioides*) [50–53]. In our transcriptome data, *p53* exhibited consistently high expression in 2nRCC, 3nRCR, and 4nAT under low-temperature, while *caspase 8* showed upregulated expression specifically in 4nAT. Activation of *caspase-3* signifies entry into the irreversible stage of apoptosis, and direct measurement of *caspase-3* activity and TUNEL assays in future work could resolve this ambiguity. Subsequent investigations will evaluate the effects of pharmacological modulation (inhibition/activation) of the NRF2 pathway on cold tolerance across ploidy variants, with particular focus on comparative analysis between the triploid 3nRCR and its diploid (RCC) and allotetraploid (4nAT) progenitors.

4.3. Immune Modulation and Metabolic Reprogramming

R Allam et al. found that the absence of NLRP3 limits TLR-induced inflammasome priming and cytokine production [54]. We speculate that the low expression of *nlrp3* in the triploid may help attenuate inflammatory responses. Consistent with regulated suppression of NLRP3 inflammasome activation, gill histological sections showed markedly fewer inflammatory cells in 3nRCR than parental strains (Figure 2H vs. Figure 2D,L). NLRP3 sense cellular damage or danger signals by forming inflammasomes and are key proteins in pyroptosis [55]. This may explain why RCC and 4nAT exhibit inflammatory responses earlier than 3nRCR, making them more susceptible to low-temperature stress. The amplified induction of *chop* (7.2-fold) and suppression of *nlrp1/nlrp3* in 3nRCR may reflect a compensatory mechanism to balance ER stress-induced apoptosis and inflammasome activation.

Analysis of the top 20 most significantly enriched pathways in 3nRCR and its parents revealed that pathways related to arginine and proline metabolism, histidine metabolism, fatty acid metabolism, retinol metabolism, and oxidative phosphorylation were enriched in 3nRCR but absent in RCC and 4nAT. These metabolic pathways may significantly contribute to its enhanced cold tolerance. Enhanced OXPHOS activity suggests improved mitochondrial efficiency, supporting ATP production essential for thermogenesis and cellular repair [56–58]. Retinol metabolism is particularly noteworthy. Retinoids (vitamin A derivatives) are potent immunomodulators and antioxidants [59]. Their upregulation in 3nRCR likely synergizes with NRF2 to bolster antioxidant defenses, mitigating cold-induced ROS (Reactive Oxygen Species) and protecting membranes and proteins. Retinol metabolism enrichment (Figure 6) synergizes with NRF2 to quench cold-induced ROS, while suppressed *nlrp3* (Figure 7) attenuates pyroptosis, redirecting energy toward stress resolution. Concurrent enrichment of arginine/proline metabolism may support polyamine synthesis (crucial for stress-responsive transcription) and nitric oxide (NO) production, influencing vasodilation, immune function, and mitochondrial biogenesis [58].

Notably, several immune-related genes (e.g., *tlr3*, *tlr5*, *nlrp1*, and *nlrp3*) were significantly modulated in 3nRCR under cold stress. While *tlr5* was upregulated—potentially enhancing bacterial surveillance [60]—the downregulation of *tlr3* and NLR inflammasome components (*nlrp1*/*nlrp3*) may mitigate excessive inflammation and pyroptosis, which are energetically costly and detrimental under cold stress [38]. This immune tuning likely facilitates resource reallocation toward cytoprotective mechanisms such as ER stress resolution and antioxidant defense, underscoring the trade-off between immune activation and metabolic homeostasis in low-temperature adaptation.

The extensive transcriptional rewiring observed in 3nRCR—with nearly 4000 DEGs—suggests that triploidy may confer enhanced genomic plasticity. Rather than being a passive consequence of genomic buffering [1], the amplified induction of *nrf2* (2.5-fold vs. 2.0-fold in RCC) implies that triploids may possess heightened basal activity or inducibility of key regulatory factors such as NRF2. This could arise from allele-specific expression or modified kinase signaling (e.g., PKR-like ER kinase) in triploids, enabling more robust activation of antioxidant and proteostatic pathways [61]. Thus, triploidy may offer a distinct regulatory milieu that optimizes stress-responsive transcription.

Furthermore, the ER stress-inflammasome crosstalk identified in triploid crucian carp may represent a conserved adaptive strategy in hybrid polyploid organisms. Given that hybrid polyploidy often confers enhanced stress resilience across plants [62,63], it would be worthwhile to investigate whether similar coordination between proteostatic maintenance and inflammatory modulation exists in other hybrid polyploid fish or aquatic species facing thermal challenges. This could provide evolutionary insights into how genome duplication and recombination events shape metabolic-immune networks for environmental adaptation.

However, this work has limitations. The identified pathways and candidate genes lack direct functional validation (e.g., via gene knockdown), and the findings remain at the mRNA level without protein confirmation and epigenetic modification. Additionally, the acute cold stress model may not fully reflect natural gradual temperature changes. Future studies should focus on functional genetic experiments and long-term acclimation mechanisms.

In summary, this study suggests that the triploid crucian carp (3nRCR) may achieve enhanced cold tolerance through a coordinated adaptive strategy involving NLRP3 inflammasome suppression, activation of the endoplasmic reticulum (ER) stress pathway, mitochondrial apoptosis and metabolic reprogramming. These convergent mechanisms are hypothesized to collectively maintain cellular homeostasis and mitigate inflammatory damage under cold stress. Our findings provide transcriptomic evidence and qPCR validation supporting a novel mechanistic basis for hybrid polyploid heterosis and highlight key genetic targets for future functional validation in breeding cold-resilient aquaculture species. This work underscores the importance of genomic plasticity in environmental adaptation and proposes a promising strategy for sustainable aquaculture development.

Supplementary Materials: The following supporting information can be downloaded at: https://www.mdpi.com/article/10.3390/fishes10100519/s1. Figure S1: Number of alternative splicing events in the liver transcriptomes of 3nRCR and its parents under cold stress; Figure S2: GO analysis of DEGs in liver tissues of 3nRCR and their parents; Figure S3: KEGG classification annotation analysis of signification DEGs in liver tissues of 3nRCR and their parents; Table S1: Primers for qPCR detection of 8DEG; Table S2: Primers for qPCR detection of 5 genes in Ko04141; Table S3: Summary of transcriptome sequencing data.

Author Contributions: S.T.: Conceptualization, Methodology, Software, Formal analysis, investigation, Data curation and Writing—original draft; Z.Z.: Writing—original draft, Writing—review and editing; S.C.: Software and Data curation; J.C.: Formal analysis; Y.W.: Formal analysis; K.L.:

Conceptualization and Methodology; W.L. (Wei Liu): Data curation and Project administration; Q.L.: Writing—review; W.L. (Wuhui Li): editing; S.L.: Funding acquisition, Writing—review and editing. All authors have read and agreed to the published version of the manuscript.

Funding: This research was supported by Yuelushan Laboratory Breeding Program (Grant No. YLS-2025-ZY01011), National Natural Science Foundation of China (Grant No. 32293252), the earmarked fund for China Agriculture Research System (Grant No. CARS-45), 111 Project (D20007), Hunan University of Chinese Medicine University-level Scientific Research Project, grant No. 2025XJZC006; Hunan University of Chinese Medicine Undergraduate Innovation and Entrepreneurship Training Program, grant No. X202410541227; Hunan University of Chinese Medicine Undergraduate Scientific Research and Innovation Fund, grant No.2024BKS099; The earmarked fund for HARS, grant number HARS-07.

Institutional Review Board Statement: All animal experiments in our study were performed in strict accordance with the legal and ethical framework of the People's Republic of China. Our entire study protocol was submitted to, reviewed, and approved by the Institutional Animal Care and Use Committee (IACUC) of Hunan normal university (no.99; 2025-03-06). All experimental procedures were conducted in strict accordance with institutional animal care guidelines. To ensure humane treatment, fish were anesthetized with 80 mg/L MS-222 (tricaine methanesulfonate) before dissection, following internationally recognized animal welfare guidelines for scientific research.

Data Availability Statement: The original contributions presented in this study are included in the supplementary material. Further inquiries can be directed to the corresponding author.

Acknowledgments: First, we extend our gratitude to the Engineering Research Center of Polyploid Fish Reproduction and Breeding of the State Education Ministry for providing the essential research conditions and a conducive academic environment for this study. We also thank our fellow students and colleagues for their valuable insights shared during discussions and exchanges, which have significantly contributed to the refinement and enhancement of this research.

Conflicts of Interest: The authors declare no conflicts of interest.

Abbreviations

The following abbreviations are used in this manuscript:

RCC	Improved diploid red crucian carp
3nRCR	triploid Xiangyun crucian carp 2
4nAT	Improved tetraploids
PFA	paraformaldehyde
H&E	hematoxylin and eosin
RIN	RNA integrity number
qRT-PCR	Quantitative Real-Time PCR
SD	standard deviation
ANOVA	one-way analysis of variance
AS	alternative splicing
DEGs	differentially expressed genes
GO	Gene Ontology
NLR	NOD-like receptor
TLR	Toll-like receptor
ER	endoplasmic reticulum
ISR	integrated stress response
IFN	interferon
LOE	Loss of equilibrium
NO	nitric oxide
ROS	Reactive Oxygen Species
OXPHOS	Oxidative Phosphorylation

References

1. Ren, L.; Zhang, X.; Li, J. Diverse transcriptional patterns of homoeologous recombinant transcripts in triploid fish (*Cyprinidae*). *Sci. China Life Sci.* **2021**, *64*, 1491–1501. [CrossRef]
2. Wang, S.; Tang, C.C.; Tao, M.; Liu, S.J. Establishment and application of distant hybridization technology in fish. *Sci. China Life Sci.* **2018**, *48*, 1310–1329. [CrossRef]
3. Brett, J.R. Energetic responses of salmon to temperature. A study of some thermal relations in the physiology and freshwater ecology of sockeye salmon (*Oncorhynchus nerkd*). *Am. Zool.* **1971**, *11*, 99–113. [CrossRef]
4. Brett, J.R. Environmental factors and growth. *Fish Physiol.* **1979**, *8*, 599–675. [CrossRef]
5. Ren, X.; Wang, Q.; Shao, H. Effects of low temperature on shrimp and crab physiology, behavior, and growth: A review. *Front. Mar. Sci.* **2021**, *8*, 746177. [CrossRef]
6. Tort, L. Stress and immune modulation in fish. *Dev. Comp. Immunol.* **2011**, *35*, 1366–1375. [CrossRef]
7. Ge, G.; Long, Y.; Shi, L. Transcriptomic profiling revealed key signaling pathways for cold tolerance and acclimation of two carp species. *BMC Genom.* **2020**, *21*, 539. [CrossRef]
8. Huang, S.; Zhao, W.; Yan, C. Elucidating the chromatin-driven transcription regulatory networks response to *Streptococcus agalactiae* infection under low temperature in Nile tilapia. *Fish Shellfish Immunol.* **2025**, *164*, 110464. [CrossRef] [PubMed]
9. Long, Y.; Ge, G.D.; Li, X.X.; Cui, Z.B. Regulation mechanisms for cold stress responses of fish. *ACTA Hydrobiol. Sin.* **2021**, *45*, 1405–1414. [CrossRef]
10. Hsieh, S.; Chen, Y.; Kuo, C. Physiological responses, desaturase activity, and fatty acid composition in milkfish (*Chaos chanos*) under cold acclimation. *Aquaculture* **2003**, *220*, 903–918. [CrossRef]
11. Wu, C.; Sun, H.; Yang, T. The tallow-enriched diet, which mainly contained stearic acid(C18:0), chance the cold tolerance capacity of Cobia (*Rachycentron canadum*) mainly contained. *Biochem. Cell. Mol. Biol.* **2009**, *13*, 23.
12. Cheng, A.C.; Cheng, S.A.; Chen, Y.Y. Effects of temperature change on the innate cellular and humoral immune responses of orange-spotted grouper *Epinephelus coioides* and its susceptibility to *Vibrio alginolyticus*. *Fish Shellfish Immunol.* **2009**, *26*, 768–772. [CrossRef]
13. Reid, C.H.; Patrick, P.H.; Rytwinski, T.; Taylor, J.J.; Willmore, W.G.; Reesor, B.; Cooke, S.J. An updated review of cold shock and cold stress in fish. *J. Fish Biol.* **2022**, *100*, 1102–1137. [CrossRef]
14. Shehata, A.I.; Shahin, S.A.; Taha, S.A. Essential Oil of Bay Laurel (*Laurus nobilis*) Enhances Growth and Immunity in Cold-Stressed Nile Tilapia (*Oreochromis niloticus*). *J. Anim. Physiol. Anim. Nutr.* **2025**, *109*, 926–941. [CrossRef] [PubMed]
15. Zhou, Y.; Li, R.X.; Lu, X.; Zhang, S. Progress in the tissue, cellular, and molecular mechanisms of cold tolerance in fish and its applications in breeding. *J. Shanghai Ocean Univ.* **2025**, *34*, 12–24. [CrossRef]
16. Zhang, Z.; Chen, J.; Li, L. Research advances in animal distant hybridization. *Sci. China Life Sci.* **2014**, *57*, 889–902. [CrossRef]
17. Liu, S.; Luo, J.; Chai, J. Genomic incompatibilities in the diploid and tetraploid offspring of the goldfish × common carp cross. *Proc. Natl. Acad. Sci. USA* **2016**, *113*, 1327–1332. [CrossRef]
18. Wang, J. Establishment of a Gynogenetic Diploid Crucian Carp (*Carassius auratus*) × Common Carp (*Cyprinus carpio*) Clone System and Studies on the Biological Characteristics of Its Derived Progeny. Ph.D. Thesis, Hunan Normal University, Changsha, China, 2010.
19. Yu, F.; Xiao, J.; Liang, X.Y.; Liu, S.; Zhou, G.; Luo, K.; Liu, Y.; Hu, W.; Wang, Y.; Zhu, Z. Rapid growth and sterility of growth hormone gene transgenic triploid carp. *Chin. Sci. Bull.* **2011**, *56*, 1679–1684. [CrossRef]
20. Xiao, J.; Fu, Y.; Zhou, W. Establishment of fin cell lines and their use to study the immune gene expression in cyprinid fishes with different ploidy in rhabdovirus infection. *Dev. Comp. Immunol.* **2018**, *88*, 55–64. [CrossRef] [PubMed]
21. Xiong, N.-X.; Ou, J.; Fan, L.-F. Blood cell characterization and transcriptome analysis reveal distinct immune response and host resistance of different ploidy cyprinid fish following *Aeromonas hydrophila* infection. *Fish Shellfish Immunol.* **2022**, *120*, 547–559. [CrossRef]
22. Gui, S.Y. Studies on Stress Resistance of Different Ploidy Crucians under Cadmium Stress. Master's Thesis, Hunan Normal University, Changsha, China, 2017.
23. Liu, W.; Wang, M.; Dai, L. Enhanced immune response improves resistance to cadmium stress in triploid crucian carp. *Front. Physiol.* **2021**, *12*, 666363. [CrossRef] [PubMed]
24. Liu, W.; Wen, Y.; Wang, M. Enhanced Resistance of Triploid Crucian Carp to Cadmiuminduced Oxidative and Endoplasmic Reticulum Stresses. *Curr. Mol. Med.* **2018**, *18*, 400–440. [CrossRef] [PubMed]
25. Soyano, K.; Mushirobira, Y. The Mechanism of Low-Temperature Tolerance in Fish. *Adv. Exp. Med. Biol.* **2018**, *1081*, 149–164. [CrossRef]
26. Ford, T.; Beitinger, T.L. Temperature tolerance in the goldfish, *Carassius auratus*. *J. Therm. Biol.* **2005**, *30*, 147–152. [CrossRef]
27. Jin S, R. Antioxidant and Metabolic Responses of Discus Fish (*Symphysodon* spp.) to Low-Temperature Stress. Master's Thesis, Shanghai Ocean University, Shanghai, China, 2019.

28. Xie, M. Effects of Low Temperature Stress on Physiology, Biochemistry and Fatty Acids in Brown-Marbled Grouper (*Epinephelus fuscoguttatus*). Master's Thesis, Guangdong Ocean University, Zhanjiang, China, 2012.
29. Ge, Y.T.; Tong, J.Y.; Li, W.; Zhou, Y.; Chen, L. Gill tissue structural changes and physiological responses of tilapia under low temperature stress. *J. South. Agric.* **2024**, *55*, 3127–3135. [CrossRef]
30. Ma, D.M.; Cheng, G.P.; Yu, H.Y.; Deng, R.Z. Study on the Mortality Response of GIFT Tilapia (*Oreochromis niloticus*) to Stress from Different Cooling Rates. *Guangxi J. Anim. Husb. Vet. Med.* **2010**, *04*, 200–202.
31. Long, Y.; Li, X.; Li, F.; Ge, G.; Liu, R.; Song, G.; Li, Q.; Qiao, Z.; Cui, Z. Transcriptional programs underlying cold acclimation of common carp (*Cyprinus carpio* L.). *Front. Genet.* **2020**, *11*, 556418. [CrossRef]
32. Fangue, N.A.; Osborne, E.J.; Todgham, A.E.; Schulte, P.M. The onset temperature of the heat-shock response and whole-organism thermal tolerance are tightly correlated in both laboratory-acclimated and field-acclimatized tidepool sculpins (*Oligocottus maculosus*). *Physiol. Biochem. Zool.* **2011**, *84*, 341–352. [CrossRef]
33. Jutfelt, F.; Roche, D.G.; Clark, T.D.; Norin, T.; Binning, S.A.; Speers-Roesch, B.; Amcoff, M.; Morgan, R.; Andreassen, A.H.; Sundin, J. Brain cooling marginally increases acute upper thermal tolerance in Atlantic cod. *J. Exp. Biol.* **2019**, *222*, jeb208249. [CrossRef]
34. Zhu, P.; Wang, G.; Liu, Y.; Wen, L.; Bo, Q.; Liu, G.; Wang, C.; Liu, B. Transcriptomic analysis reveals the molecular mechanisms of heterosis in low-temperature tolerance in the hybrids of *Argopecten* scallops. *Comp. Biochem. Physiol. Part D Genom. Proteom.* **2025**, *55*, 101526. [CrossRef]
35. Sollid, J.; KJernsli, A.; de Angelis, P.M.; Rohr, A.K.; Nilsson, G.E. Cell proliferation and gill morphology in anoxic crucian carp. *Am. J. Physiol.—Regul. Integr. Comp. Physiol.* **2005**, *289*, R1196–R1201. [CrossRef]
36. Sollid, J.; Nilsson, G.E. Plasticity of respiratory structures—Adaptive remodeling of fish gills induced by ambient oxygen and temperature. *Respir. Physiol. Neurobiol.* **2006**, *154*, 241–251. [CrossRef]
37. Schröder, M. Endoplasmic reticulum stress responses. *Cell. Mol. Life Sci.* **2008**, *65*, 862–894. [CrossRef]
38. Yang, Q.; Yu, C.; Yang, Z. Deregulated NLRP3 and NLRP1 inflammasomes and their correlations with disease activity in systemic lupus erythematosus. *J. Rheumatol.* **2014**, *41*, 444–452. [CrossRef]
39. Shore, G.C.; Papa, F.R.; Oakes, S.A. Signaling cell death from the endoplasmic reticulum stress response. *Curr. Opin. Cell Biol.* **2011**, *23*, 143–149. [CrossRef] [PubMed]
40. Yuan, S.L. Molecular Mechanism of GCN2 Signaling Pathway Regulating Rapid Growth of Triploid Crucian Carp. Master's Thesis, Hunan Normal University, Changsha, China, 2021.
41. Wang, W.; Gao, X.; Liu, L.; Guo, S.; Duan, J.; Xiao, P. Zebrafish as a vertebrate model for high-throughput drug toxicity screening: Mechanisms, novel techniques, and future perspectives. *Journal of Pharmaceutical Analysis* **2025**, *15*, 101195. [CrossRef]
42. Hai, H.; Ming-Xing, T.; Chan, D. Mechanisms of CHOP regulating endoplasmic reticulum stress-mediated apoptosis. *Chin. J. Prev. Vet. Med.* **2019**, *41*, 219.
43. Huang, S.; Yan, C.; Hu, P. Chromatin dynamics and transcriptional regulation of heat stress in an ectothermic fish. *Proc. B* **2025**, *292*, 20250769. [CrossRef]
44. Todd, D.J.; Lee, A.-H.; Glimcher, L.H. The endoplasmic reticulum stress response in immunity and autoimmunity. *Nat. Rev. Immunol.* **2008**, *8*, 663–674. [CrossRef]
45. Kim, E.M.; Jung, C.-H.; Kim, J. The *p53/p21* complex regulates cancer cell invasion and apoptosis by targeting Bcl-2 family proteins. *Cancer Res.* **2017**, *77*, 3092–3100. [CrossRef]
46. Lubawy, J.; Chowański, S.; Adamski, Z.; Słocińska, M. Mitochondria as a target and central hub of energy division during cold stress in insects. *Front. Zool.* **2022**, *19*, 1. [CrossRef] [PubMed]
47. Dzik, K.P.; Majkutewicz, I.; Kołodziej, M.; Gorlikowska, K.; Nekrash, M.; Kaczor, J.J. Impact of cold exposure duration and intensity on hippocampal tyrosine hydroxylase, brain-derived neurotrophic factor, and mitochondrial markers in mice. *Exp. Neurol.* **2025**, *393*, 115407. [CrossRef] [PubMed]
48. Sun, S.; Cao, X.; Gao, J. C24: 0 avoids cold exposure-induced oxidative stress and fatty acid β-oxidation damage. *Iscience* **2021**, *24*, 103409. [CrossRef] [PubMed]
49. Liu, T.; Li, L.; Liu, H. Effects of chronic cold stress and thermal stress on growth performance, hepatic apoptosis, oxidative stress, immune response and gut microbiota of juvenile hybrid sturgeon (*Acipenser baerii* ♀× *A. schrenkii* ♂). *Fish Shellfish Immunol.* **2025**, *157*, 110078. [CrossRef]
50. Liu, R.; Liu, R.; Song, G.; Li, Q.; Cui, Z.; Long, Y. Mitochondria dysfunction and cell apoptosis limit resistance of Nile Tilapia (*Oreochromis niloticus*) to lethal cold stress. *Animals* **2022**, *12*, 2382. [CrossRef]
51. Cheng, C.-H.; Ye, C.-X.; Guo, Z.-X.; Wang, A.-L. Immune and physiological responses of pufferfish (*Takifugu obscurus*) under cold stress. *Fish Shellfish Immunol.* **2017**, *64*, 137–145. [CrossRef]
52. Li, Y.; Huang, J.S.; Chen, Y.M. Effects of low temperature stress on antioxidant capacity, cell apoptosis, and tissue structure in gill of juvenile cobia (*Rachycentron canadum*). *South China Fish. Sci.* **2023**, *19*, 68–77.
53. Sun, Z.; Tan, X.; Liu, Q.; Ye, H.; Zou, C.; Xu, M.; Zhang, Y.; Ye, C. Physiological, immune responses and liver lipid metabolism of orange-spotted grouper (Epinephelus coioides) under cold stress. *Aquaculture* **2019**, *498*, 545–555. [CrossRef]

54. Allam, R.; E Lawlor, K.; Yu, E.C.; Mildenhall, A.L.; Moujalled, D.M.; Lewis, R.S.; Ke, F.; Mason, K.D.; White, M.J.; Stacey, K.J.; et al. Mitochondrial apoptosis is dispensable for NLRP 3 inflammasome activation but non-apoptotic *caspase-8* is required for inflammasome priming. *EMBO Rep.* **2014**, *15*, 982–990. [CrossRef]
55. Antonopoulos, C.; Russo, H.M.; El Sanadi, C. Caspase-8 as an effector and regulator of NLRP3 inflammasome signaling. *J. Biol. Chem.* **2015**, *290*, 20167–20184. [CrossRef]
56. Itoi, S.; Kinoshita, S.; Kikuchi, K. Changes of carp FoF1-ATPase in association with temperature acclimation. *Am. J. Physiol.-Regul. Integr. Comp. Physiol.* **2003**, *284*, 152–163. [CrossRef] [PubMed]
57. Wodtke, E. Temperature adaptation of biological membranes. The effects of acclimation temperature on the unsaturation of the main neutral and charged phospholipids in mitochondrial membranes of the carp (*Cyprinus carpio* L.). *Biochim. Et Biophys. Acta (BBA)-Biomembr.* **1981**, *640*, 698–709. [CrossRef]
58. Liang, L.; Chang, Y.; He, X. Transcriptome analysis to identify cold-responsive genes in amur carp (*Cyprinus carpio haematopterus*). *PLoS ONE* **2015**, *10*, e0130526. [CrossRef]
59. Meyer, E.; Lamote, I.; Burvenich, C. Retinoids and steroids in bovine mammary gland immunobiology. *Livest. N Prod. Sci.* **2005**, *98*, 33–46. [CrossRef]
60. Applequist, S.E.; Wallin, R.P.A.; Ljunggren, H. Variable expression of Toll-like receptor in murine innate and adaptive immune cell lines. *Int. Immunol.* **2002**, *14*, 1065–1074. [CrossRef]
61. Cano, M.; Datta, S.; Wang, L.; Liu, T.; Flores-Bellver, M.; Sachdeva, M.; Sinha, D.; Handa, J.T. Nrf2 deficiency decreases NADPH from impaired IDH shuttle and pentose phosphate pathway in retinal pigmented epithelial cells to magnify oxidative stress-induced mitochondrial dysfunction. *Aging Cell* **2021**, *20*, e13444. [CrossRef]
62. Li, X.; Zhang, L.; Wei, X.; Datta, T.; Wei, F.; Xie, Z. Polyploidization: A Biological Force That Enhances Stress Resistance. *Int. J. Mol. Sci.* **2024**, *25*, 1957. [CrossRef]
63. Tossi, V.E.; Tosar, L.J.M.; Laino, L.E.; Iannicelli, J.; Regalado, J.J.; Escandón, A.S.; Baroli, I.; Causin, H.F.; Pitta-Álvarez, S.I. Impact of polyploidy on plant tolerance to abiotic and biotic stresses. *Front. Plant Sci.* **2022**, *13*, 869423. [CrossRef] [PubMed]